



ELSEVIER

Contents lists available at ScienceDirect

## Journal of Magnetism and Magnetic Materials

journal homepage: [www.elsevier.com/locate/jmmm](http://www.elsevier.com/locate/jmmm)

## Endothelial biocompatibility and accumulation of SPION under flow conditions

Jasmin Matuszak<sup>a</sup>, Jan Zaloga<sup>a</sup>, Ralf P. Friedrich<sup>a</sup>, Stefan Lyer<sup>a</sup>, Johannes Nowak<sup>b</sup>, Stefan Odenbach<sup>b</sup>, Christoph Alexiou<sup>a</sup>, Iwona Cicha<sup>a,\*</sup><sup>a</sup> Section of Experimental Oncology and Nanomedicine (SEON), Else Kröner-Fresenius Stiftungsprofessur for Nanomedicine, University Hospital Erlangen, Erlangen, Germany<sup>b</sup> Chair of Magnetofluidynamics, Measuring and Automation Technology, Technische Universität Dresden, Dresden, Germany

## ARTICLE INFO

## Article history:

Received 30 June 2014

Received in revised form

15 August 2014

Accepted 2 September 2014

Available online 10 September 2014

## Keywords:

Atherosclerosis

Magnetic nanoparticle

Endothelial cell

SPION uptake

Biocompatibility

Live-cell analysis

## ABSTRACT

Magnetic targeting is considered a promising method to accumulate the nanoparticles at the sites of atherosclerotic lesions, but little is known about the biological effects of magnetic nanoparticles on the vascular wall. Here, we investigated endothelial cell growth and vitality upon treatment with SPION (0–60 µg/mL) using two complementing methods: real-time cell analysis and live-cell microscopy. Moreover, the uptake of circulating superparamagnetic iron oxide nanoparticles (SPIONs) was assessed in an *in vitro* model of arterial bifurcations.

At the tested concentrations, SPIONs were well tolerated and had no major influence on endothelial cell growth. Our results further showed a uniform distribution of endothelial SPION uptake independent of channel geometry or hemodynamic conditions: In the absence of magnetic force, no increase in accumulation of SPIONs at non-uniform shear stress region at the outer walls of bifurcation was observed. Application of external magnet allowed enhanced accumulation of SPIONs at the regions of non-uniform shear stress. Increased uptake of SPIONs at non-uniform shear stress region was well tolerated by endothelial cells (ECs) and did not affect endothelial cell viability or attachment. These findings indicate that magnetic targeting can constitute a promising and safe technique for the delivery of imaging and therapeutic nanoparticles to atherosclerotic lesions.

© 2014 Elsevier B.V. All rights reserved.

## 1. Introduction

Atherosclerosis and the resulting cardiovascular syndromes are the major cause of death worldwide and remain one of the biggest global health problems [1]. Although both the understanding of the disease mechanisms and the imaging techniques for atherosclerotic plaque detection have considerably advanced, more efficient therapies are still needed. Currently, many pharmacological substances for the treatment of clinical manifestations of atherosclerosis are on the market, but their systemic delivery has significant disadvantages, such as severe side effects and low efficacy at tolerated doses. Furthermore, interventional techniques like stent implantation necessitate the long-lasting antiplatelet therapy and may lead to in-stent restenosis [2]. A novel promising method to overcome the

disadvantages of existing cardiovascular therapies is magnetic drug targeting [3–7]. The idea is to link SPIONs with anti-atherosclerotic drugs and then accumulate these magnetic drug carriers at the site of atherosclerotic lesion. The amount of pharmacological agents needed for sufficient treatment could be dramatically reduced if the drug-carrying nanoparticles are directly targeted at the plaque, which would decrease the systemic side effects and improve the treatment outcome reviews [8,9]. However, for this purpose, a substantial amount of preclinical studies is necessary to analyze the biological effects of magnetic nanoparticles on the vascular wall. So far, little is known about possible interactions between magnetic nanoparticles and the vascular cells, although some contradicting reports regarding endothelial toxicity of iron oxide nanoparticles in static cell culture were recently published [10,11]. Therefore, our aim was to investigate the effects of SPIONs on endothelial cells, which are the first contact cells for circulating nanoparticles. Furthermore, we used an *in vitro* arterial bifurcation model in combination with a peristaltic pump, which imitates physiologic blood flow, to analyze the endothelial accumulation of circulating SPIONs, with or without external magnetic force.

\* Correspondence to: Cardiovascular Nanomedicine Unit, Section of Experimental Oncology and Nanomedicine, ENT Department, University of Erlangen-Nuremberg, Glückstr. 10a, 91054 Erlangen, Germany. Tel.: +49 9131 8543953; fax: +49 9131 8534282.

E-mail address: [Iwona\\_Cicha@yahoo.com](mailto:Iwona_Cicha@yahoo.com) (I. Cicha).

## 2. Materials and methods

### 2.1. Materials

Cell culture reagents and media were obtained from Promo Cell (Heidelberg, Germany). Accutase™ was from PAA Laboratories (Linz, Austria) and dispase from Life Technologies GmbH (Darmstadt, Germany).

### 2.2. Nanoparticles

Lauric acid-coated SPIONs (SPION<sup>LAU</sup>) were synthesized at SEON as previously described [7]. Prior to their use in cell culture studies, the SPIONs were stabilized by incubation 1:1 with a freshly prepared 10% bovine serum albumin (BSA) solution (Merck, 1.12018) and sterilized by filtration through a 0.2 μm CME syringe filter (Roth, Germany). The lauric acid-coated, BSA-stabilised nanoparticles are for simplicity referred to as SPIONs further in the text.

### 2.3. Nanoparticle characterization

For nanoparticle characterization, hydrodynamic diameter, zeta potential and saturation magnetization of SPIONs were measured. Furthermore, the colloidal stability of SPIONs in cell culture medium and human blood was tested. Measurements of size were performed in triplicate using Nanophox (Sympatec, Clausthal-Zellerfeld, Germany) on the SPION suspension diluted to an iron concentration of 25 μg/mL with distilled water or cell culture medium. Zeta potential of SPIONs in distilled water or cell culture medium was measured with a NICOMP 380ZLS (Nicomp, Port Richey, FL, USA) at an iron concentration of 25 μg/mL.

Transmission electron microscopy (TEM) pictures were taken with a CM 300 UltraTWIN (Philips, Eindhoven, Netherlands) operated at an acceleration voltage of 300 kV. Samples were prepared by drying 10 μL of diluted nanoparticle suspension on a carbon-coated Athene S147-2 copper grid (Plano, Wetzlar, Germany).

The magnetization curves were measured in triplicate using the vibrating sample magnetometer (VSM) Lake Shore 7407 (LakeShoreCryotronics Inc., Westerville, USA). The external magnetic field was constantly increased while the magnetization of the sample was measured. As the spontaneous magnetization of the core material (assumed as magnetite here) is known, the resulting magnetization curves allowed calculation of the saturation magnetization  $M_S$  leading to the volume fraction of magnetic material  $\phi$ .

For examination of colloidal stability in cell culture medium and blood, SPION and SPION<sup>LAU</sup> (coated with lauric acid only, without BSA) were added to medium and to freshly collected heparin-anticoagulated human whole blood to an iron concentration of 1.54 mg/mL. After 1 h incubation, 2 μL of respective samples were placed on a glass slide and analyzed for nanoparticle aggregates with a Zeiss Axio observer Z1 microscope (Zeiss Optics, Jena, Germany).

### 2.4. Cell culture

Human umbilical vein endothelial cells (HUVECs) were isolated from freshly collected umbilical cords (kindly provided by the Dept. of Gynaecology, University Hospital Erlangen) using an established technique. The use of human material was approved by the local ethics committee at the University Hospital Erlangen. Cells were cultured in Endothelial Cell Growth Medium (ECGM, PromoCell, Heidelberg, Germany) with endothelial cell growth supplement containing 5% fetal calf serum, 4 μL/mL heparin, 10 ng/mL epidermal growth factor, 1 μg/mL hydrocortisone, 50 μg/mL gentamycin sulfate, and 50 ng/mL amphotericin B, at humidified 5% CO<sub>2</sub> atmosphere. In all experiments, HUVECs at passage 1–2 were used.

### 2.5. Flow cytometry

Flow cytometry was employed to clarify the potential toxicity of SPION treatment on endothelial cells. For that purpose, 0.1–0.2 × 10<sup>5</sup> HUVECs were seeded in 24-well plates and grown overnight. Subsequently, the culture medium was replaced by medium supplemented with SPIONs at 10, 30 and 60 μg/mL. As control, medium without SPIONs was used. Cells were incubated for 24 h and 48 h, after which the supernatants containing detached dead cells were collected for each well. Adherent viable cells were subsequently harvested and added to the supernatants. After centrifugation, cells were stained with propidium iodide to identify necrotic cells (Sigma), and nuclear dye Hoechst 33342 (Life Technologies) to discriminate between cells and nanoparticles. Fluorescence was measured with flow cytometer (Gallios, Beckman Coulter, Fullerton, USA). Electronic compensation was used to eliminate bleed through fluorescence.

### 2.6. Live-cell microscopy

HUVECs were seeded in 96-well plates at 2 × 10<sup>3</sup> cells/well in 100 μL medium. At 24 h after seeding, additional 100 μL of media containing different concentrations of nanoparticles were added to the wells as follows: (a) for controls, 100 μL of pure medium without nanoparticles, and (b) for the treatment samples, 100 μL of medium containing NPs at the concentration 2 × higher than the required end-concentration. The resulting end volume for each well was 200 μL. Cell growth was monitored for subsequent 72 h using live cell-imager (Incucyte FLR microscope system, Essen Bioscience, AnnArbor, USA) placed in a humidified incubator with 37 °C and 5% CO<sub>2</sub>. The experiments were performed in duodecuplicate (12 wells per each nanoparticle concentration).

### 2.7. Real-time cell analysis

For monitoring the effects of nanoparticles on HUVEC viability, the xCELLigence system (RTCA DP Analyzer, Roche Diagnostics, Mannheim, Germany) was used. The system was placed in a humidified incubator with 37 °C and 5% CO<sub>2</sub>. Experiments were performed in 16-well E-plates (ACEA Bioscience, San Diego, USA), in which the impedance is measured with the help of microelectrodes localized at the bottom of the wells. For the background measurement, 100 μL of cell-free endothelial cell growth medium was added to the wells. Afterwards, 50 μL of media from each well were replaced with 50 μL of cell suspension containing 1 × 10<sup>3</sup> HUVECs. The experiments were performed in hexaplicate.

About 30 min after seeding of the cells, the monitoring of impedance by the xCELLigence system was started. At 24 h after seeding, additional 100 μL of media containing different concentrations of nanoparticles were added to the wells as follows: (a) for controls, 100 μL of pure medium without nanoparticles, and (b) for the treatment samples, 100 μL of medium containing NPs at the concentration 2 × higher than the required end-concentration. The resulting end volume for each well was 200 μL. The “cell-index”, reflecting the numbers, adherence and viability of cells, was monitored every 10 min for 96 h.

### 2.8. Bifurcation model

The bifurcating flow-through cell culture slides suitable for direct microscopic studies were obtained from Ibidi® (y-shaped μ-slides, Munich, Germany). Numerical flow simulation performed in our previous study [12], distinguished the region of laminar shear stress throughout the straight main channel, characterized by high shear stress 10.2–10.8 dyne/cm<sup>2</sup>, strictly laminar pattern with nearly parallel streamlines, and the region of non-uniform shear stress at the outer walls of bifurcation, characterized by

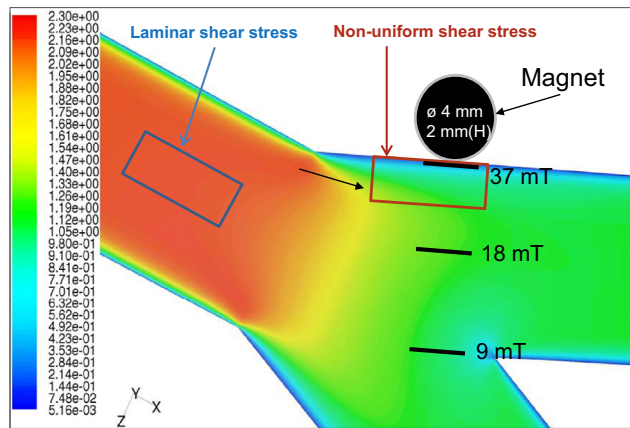


**Fig. 1.** The model of bifurcations and experimental setup. Wall shear stress pattern in bifurcating slides, color scale in Pa (1 Pa=10 dyne/cm<sup>2</sup>), regions of laminar or non-uniform shear stress are indicated. Schematic presentation of magnet placement for the targeted accumulation of nanoparticles and the magnetic flux density measured with a tesla-meter are shown.

reduced flow rate and perturbed shear pattern, with steep shear stress gradient in transversal direction to flow (shear stress range from  $\sim 6.3$  dyne/cm<sup>2</sup> to  $\sim 0.5$  dyne/cm<sup>2</sup>) [12].

## 2.9. Flow experiments

For the flow experiments, HUVECs at  $7 \times 10^5$  /mL were seeded in the bifurcating slides and grown until confluence. Using a programmed peristaltic pump (Ismatec), cell monolayer inside the slide channel was perfused with medium (with or without nanoparticles) at arterial shear stress (10 dyne/cm<sup>2</sup>, corresponding to flow rate of 9.6 mL/min) for 18 h. For the perfusion with nanoparticles, 2 different concentrations were used: 30  $\mu$ g/mL and 3  $\mu$ g/mL. For 3  $\mu$ g/mL, a magnet was positioned directly at the outer wall of the bifurcation to test accumulation of particles (Fig. 1).

After 18 h, slides were detached from the pump system, washed with phosphate buffered saline (PBS) and fixed with 4% formalin for 10 min at room temperature (RT). After subsequent washing with PBS, particles were stained with Prussian blue (1:1 potassium ferrocyanide (2%) and hydrochloric acid (2%)) for 30 min at RT and washed afterwards several times with distilled water. Nuclei of the cells were counterstained with nuclear fast-red (Merck, Darmstadt, Germany) for 10 min at RT, followed by rinsing with distilled water and repeated washing with 100% of ethanol. As a mounting medium, Mowiol (Roth, Karlsruhe, Germany) was added to extend staining durability.

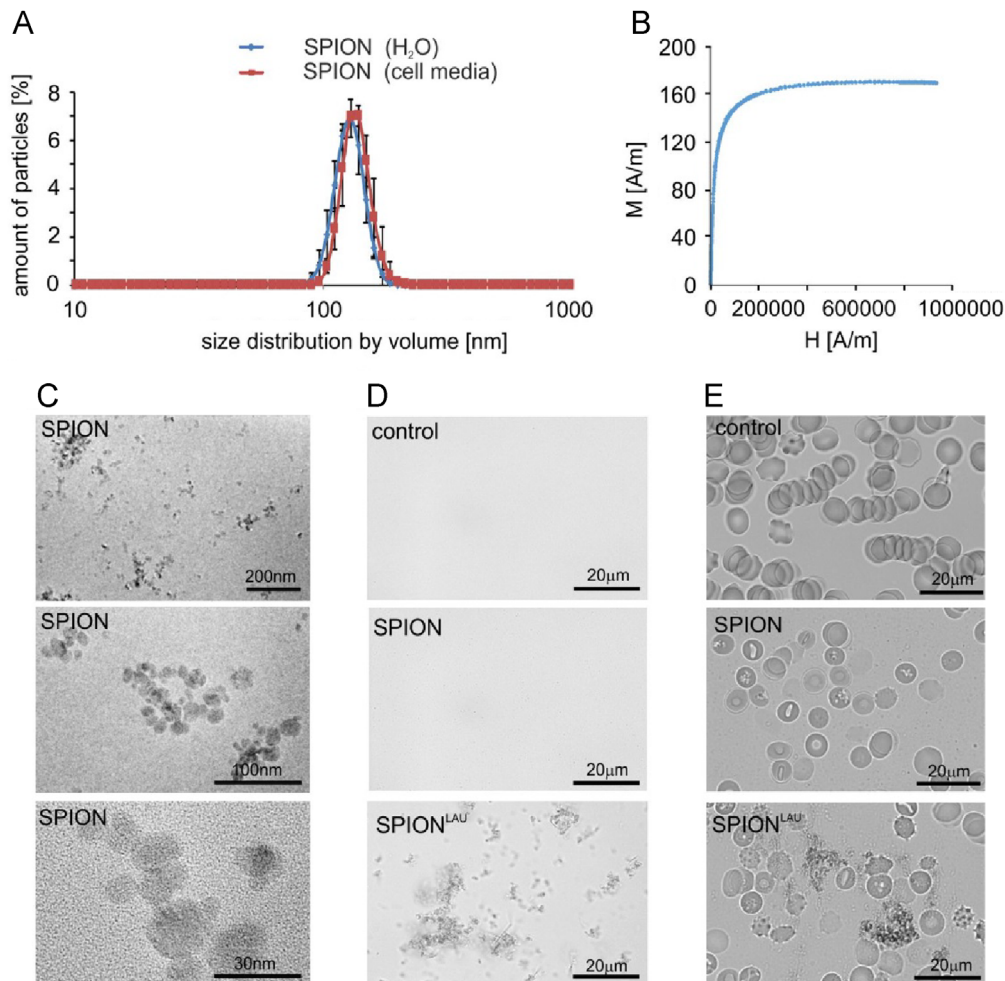


**Fig. 2.** Nanoparticle characterization: (A) Average hydrodynamic diameter was measured with DLS in water and cell culture medium; (B) saturation magnetization was measured with VSM; (C) TEM images of SPIONs; (D) microscopic images of colloidal stability of SPION in cell culture medium after 1 h. Control is medium alone; and (E) microscopic images of colloidal stability in human blood after 1 h. Control is blood alone.

## 2.10. Statistical analyses

The SigmaPlot<sup>®</sup> Software was used for statistical analyses. Data are expressed as mean  $\pm$  SEM, unless stated otherwise.  $P < 0.05$  was considered statistically significant.

## 3. Results and discussion:

### 3.1. Nanoparticle characterization and stability in biological fluids

According to the dynamic light scattering measurements, the average hydrodynamic diameter of SPIONs in distilled water was 126.3 nm (Fig. 2A), and their charge was negative ( $-34.56$  mV). In cell culture medium, the average hydrodynamic diameter increased slightly to 134.4 nm and the absolute value of charge decreased to around zero ( $-0.13$  mV). The magnetization curves measured with the VSM, are depicted in Fig. 2B. The samples show superparamagnetic behavior. The saturation magnetization  $M_S$  calculated from magnetization curves was 174.80 A/m resulting in the volume fraction of magnetic material  $\phi = 0.039\%$ .

In order to assess the stability of nanoparticles in complex biological fluids, the BSA-stabilized SPIONs and SPION<sup>Lau</sup> without BSA (serving as additional control) were added to medium and to freshly collected human whole blood. Under the light microscope, nanoparticle aggregates were observed in the medium and blood samples containing SPION<sup>Lau</sup>, but not in SPION samples or control (untreated) samples (Fig. 2E and F). As the detection limit of the light microscope lies about 300–400 nm, we concluded that no major aggregates above that size had formed in the samples treated with SPIONs, indicating good nanoparticle stability.

### 3.2. Effect of SPIONs on endothelial cell growth and viability

The potential toxicity of nanoparticles is the most important concern that must be excluded prior to their application in medicine. Therefore, we first investigated whether any significant toxic effects are exerted by SPIONs on primary HUVECs *in vitro* using flow cytometry. The results of propidium iodide staining showed that the numbers of necrotic cells were not significantly different between untreated control cells and SPION-treated samples (data not shown).

To further investigate SPION effects in real-time, endothelial cell growth and vitality was assessed in parallel using two complementing methods: real-time cell analysis and live-cell microscopy.

Real-time cell analysis is a well-established method, frequently used in our group for nanotoxicity studies [13]. The “cell-index” measured with real-time cell analysis, reflecting the numbers, adherence and viability of cells, showed a steady increase over time in control cells, as well as in the cells treated with 10 or 30  $\mu\text{g}/\text{mL}$  SPIONs (Fig. 3). There were no significant differences in the growth curves of these cells against control samples, showing a similar increase of cell index until the end of the measurement at 72 h post-application. In cells treated with 60  $\mu\text{g}/\text{mL}$  SPIONs, a significantly lower cell-index in comparison to control was observed already at 24 h post-application, and at 72 h of treatment, it was 50% lower than in control samples. In spite of this, the cell indices of samples treated with 60  $\mu\text{g}/\text{mL}$  SPIONs continued to increase, albeit slower than control.

To exclude the direct influence of SPION on the impedance values, additional measurements were performed on wells containing SPIONs without the cells. Medium alone resulted in a cell-index around 0.1, a value which is negligible compared to cell-indices measured in presence of cells (usually between 2 and 3 after 72 h). The impedance measurements in SPION-containing

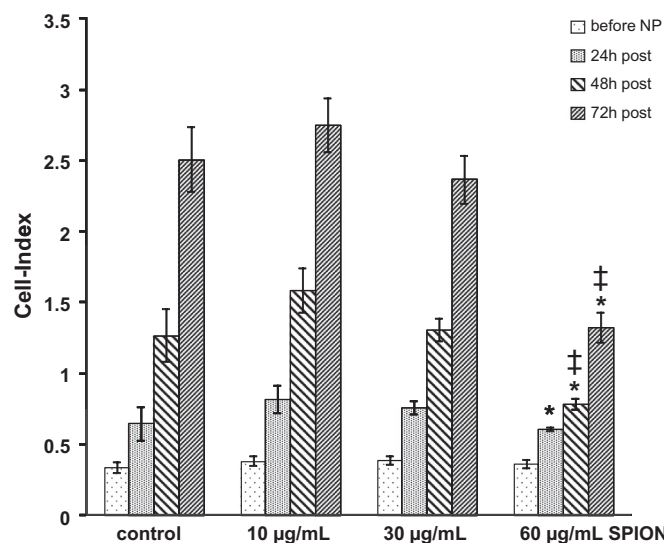


**Fig. 3.** Effect of SPIONs on primary HUVECs assessed by real-time cell analysis: In xCELLigence real-time cell analysis system, cells were seeded 24 h before nanoparticle application. After these initial 24 h, SPIONs in different concentrations were added and cell index was monitored every 10 min for 72 h post-application;  $n=3$  (each sample measured in hexuplicate). Data are expressed as mean  $\pm$  SEM. \* $p < 0.05$  versus control; † $p < 0.05$  versus 10 and 30  $\mu\text{g}/\text{mL}$  (one-way ANOVA).

medium resulted in cell-index values near zero, which were constant over time and independent of the used SPION concentrations (not shown). However, this slight negative effect could not significantly influence our measurements, as the nanoparticles do not come in direct contact with the electrodes at the bottom of the wells in the normal experimental set up.

The results of real-time analysis were validated using live-cell microscopy with the IncuCyte FLR system. In contrast to real-time cell analysis which estimates cell numbers, attachment and viability based on the impedance measurements across the bottom of the wells, live-cell microscopy allows the observation of cell morphology, and the measurement of confluence at the same time. Using this method, no differences were observed in confluence or morphology between untreated cells and the cells treated with different concentrations of SPIONs (Fig. 4).

These data underscore the importance of applying different methods to assess the toxicity of nanoparticles, as using one single method increases the risk of bias. In our case, the impedance measurements indicated a negative effect of SPIONs at 60  $\mu\text{g}/\text{mL}$  on HUVECs, because cell-index was significantly lower in comparison to control. This alone might have hinted to an impaired endothelial cell proliferation at 60  $\mu\text{g}/\text{mL}$  SPIONs, but considered side by side with the results of live-cell microscopy, indicated that it is the weaker adherence of the cells treated with 60  $\mu\text{g}/\text{mL}$ , rather than reduced cell numbers, that is responsible for the measured impedance differences.

Taken together, the results of real-time cell analysis and live-cell microscopy indicated that there was no severe toxic effect of SPIONs on HUVECs. Because of the biological effects observed at 60  $\mu\text{g}/\text{mL}$ , the concentration of 30  $\mu\text{g}/\text{mL}$  of SPION was chosen for the further studies in flow conditions.

### 3.3. An external magnetic force allows targeted SPION accumulation at bifurcations

Non-uniform shear stress at the outer walls of bifurcations induces a pro-atherogenic endothelial phenotype and increases endothelial permeability, thus promoting atherosclerotic plaque formation. We therefore investigated if nanoparticle accumulation is spontaneously increased in the non-uniform shear stress region

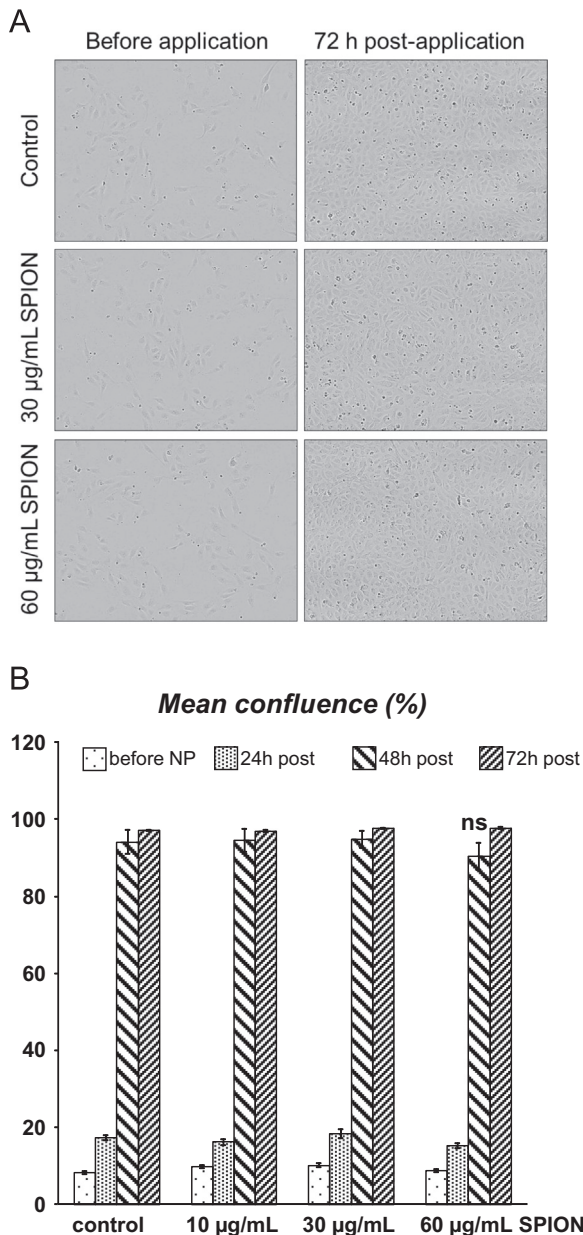


**Fig. 4.** Live-cell microscopy of HUVECs treated with SPIONs: Cells were seeded 24 h before nanoparticle application. After these initial 24 h, SPIONs in different concentrations were added and the phase contrast images were taken every hour for 72 h post-application. (A) Photos show HUVECs before and 72 h after SPION application, (B) mean confluence at the different time points;  $n=2$  (each sample measured in duodecuplicate). Data are expressed as mean  $\pm$  SEM; ns, not significant versus other tested concentrations (one-way ANOVA).

*in vitro*, as described for the spontaneous *in vivo* accumulation of LDL particles in these regions [14]. For this purpose, we seeded the endothelial cells in the bifurcating flow-through cell culture slides, which simulate the non-uniform shear stress gradient at arterial bifurcations [12]. Using this well characterized system [15,16], we perfused HUVEC monolayer with medium containing 30  $\mu\text{g}/\text{mL}$  of SPIONs for 18 h and subsequently compared the nanoparticle uptake by cells exposed to different types of shear stress (laminar versus non-uniform shear stress, see Fig. 2). Contrary to our expectations, there were no regional differences in the uptake of circulating SPIONs by HUVECs. The Prussian blue staining revealed a uniform iron accumulation in endothelial cells independent of the type of shear stress (Fig. 5, middle panel).

Next, we investigated if it is possible to accumulate SPIONs at the outer wall of bifurcation using an external magnet. For this purpose, the endothelial cell monolayer inside the bifurcating slides was perfused with medium containing 3  $\mu\text{g}/\text{mL}$  SPIONs, whereby an external magnet was placed at 1 mm distance from the outer wall of bifurcation (left branch). In the presence of external magnetic force it was possible to accumulate a large proportion of nanoparticles in the non-uniform shear stress region (Fig. 5, lower panel). At the same time, the nanoparticle uptake by HUVECs was dramatically reduced in (a) the laminar shear stress region, and (b) the branch without the magnet. Importantly, the increased uptake of SPIONs at non-uniform shear stress region was well tolerated by the cells and did not affect endothelial cell viability and morphology, nor induced cell detachment due to shear stress exposure.

These results have important implications for potential application of magnetic nanoparticles as anti-atherogenic drug carriers. Accumulation of the circulating SPIONs with the help of external magnetic force at the region of atherosclerotic plaque will allow drug dose reduction and more efficient treatment of atherosclerosis. Furthermore, as fewer drug-loaded nanoparticles will be taken up by endothelium in the laminar region, less systemic side effects are expected.

#### 4. Conclusions

SPIONs were well tolerated by endothelial cells, and did not induce major toxic effects *in vitro* up to the highest tested concentration of 60  $\mu\text{g}/\text{mL}$ . Magnetic targeting allowed a localized accumulation of increased amount of SPIONs at the region of interest under physiologic-like flow conditions, thus enabling a substantial reduction of the applied dose. These findings indicate a favorable biocompatibility profile of the used SPIONs and their potential for cardiovascular drug targeting applications.

#### 5. Outlook

Development of novel diagnostic and therapeutic nanoparticles is one of the most urgent tasks in cardiovascular medicine. The SPION concentrations selected for this study are relevant for the potential biomedical applications. In the animal model of tumor, the concentrations of 45–60  $\mu\text{g}/\text{mL}$  of blood are used for magnetic drug targeting purposes [4,7]. In humans, the maximal dose of iron oxide-based contrast agent ferumoxtran is 2.6 mg/kg, which adjusted for the blood volume of 77 mL/kg gives the concentration of 33  $\mu\text{g}/\text{mL}$ , which is within the range used in our study.

For the clinical applications, a detailed characterization of the biological responses elicited by the nanosystems *in vitro* and *in vivo* is critical. Therefore, in the future studies, we plan to investigate the effects of SPIONs on the endothelium-inflammatory cell interactions, which play a crucial role in the development and progression of atherosclerosis. Furthermore, preclinical studies *ex vivo* will be performed to standardize the magnetic field parameters for cardiovascular applications [17]. In animal model, the biodistribution of the SPIONs after magnetic targeting to atherosclerotic plaques will be examined with magnetorelaxometry, a technique which was previously used to verify the increased accumulation of nanoparticles in the region of interest after intra-arterial application combined with magnetic targeting, compared to intravenous administration [18]. These investigations, constituting an essential part of nanotoxicology and *in vivo* safety assessment, are necessary before our nanoparticles are considered for clinical use.

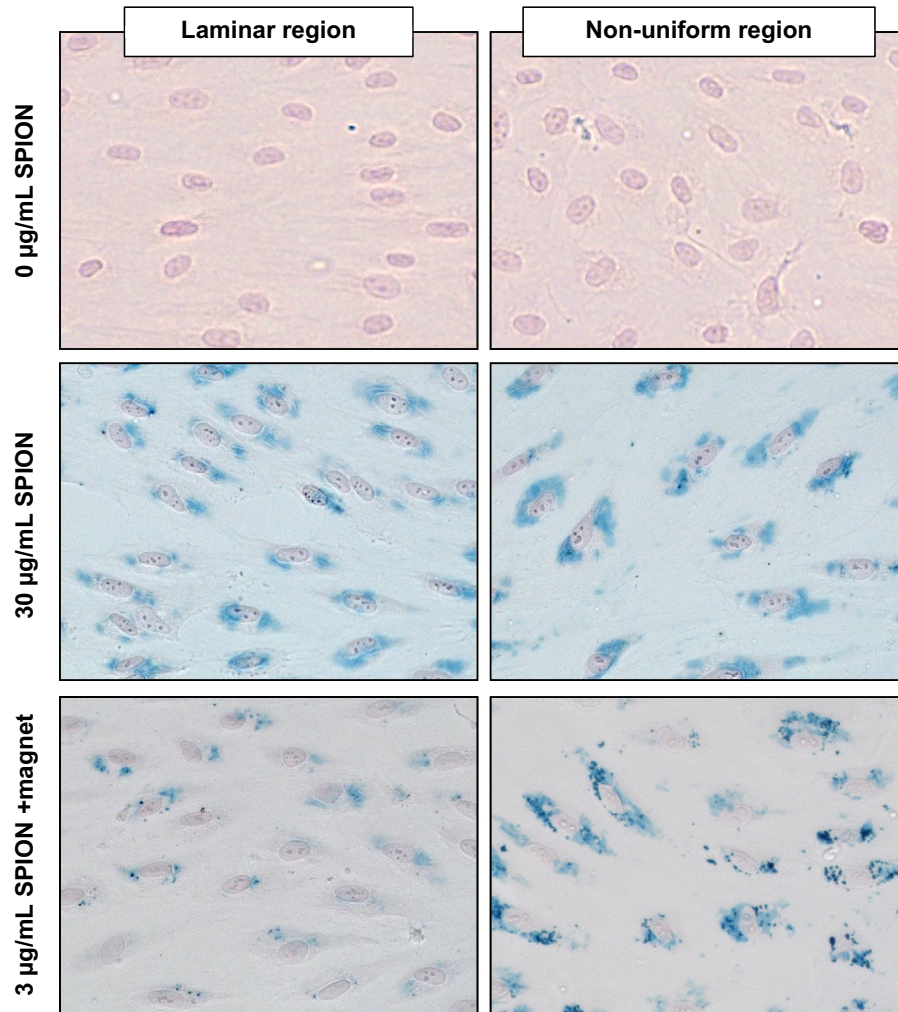


**Fig. 5.** Increased accumulation of SPIONs at the regions of non-uniform shear stress by external magnet: HUVECs were perfused for 18 h with medium containing SPIONs without external magnetic force (30 µg/mL, middle panel) or with external magnetic force (3 µg/mL, lower panel). Medium without SPIONs served as control. After PFA fixation, SPIONs were detected with Prussian blue and nuclei were counterstained with nuclear fast-red;  $n=3$ .

## Acknowledgments

This study was supported by the DFG (Grants CI 162/2-1, AL 552/5-1, and SPP1681) and the FP7-NMP-2012-LARGE-6-309820 “NanoAthero”. The authors thank Prof. Beckmann (Dept. of Gynaecology, University Hospital Erlangen, Germany) for providing umbilical cords and Nina Jaziri for help with HUVEC isolation.

## References

- [1] A.S. Go, D. Mozaffarian, V.L. Roger, E.J. Benjamin, J.D. Berry, M.J. Blaha, S. Dai, E.S. Ford, C.S. Fox, S. Franco, H.J. Fullerton, C. Gillespie, S.M. Hailpern, J.A. Heit, V.J. Howard, M.D. Huffman, S.E. Judd, B.M. Kissela, S.J. Kittner, D.T. Lackland, J.H. Lichtman, L.D. Lisabeth, R.H. Mackey, D.J. Magid, G.M. Marcus, A. Marelli, D.B. Matchar, D.K. McGuire, E.R. Mohler III, C.S. Moy, M.E. Mussolino, R.W. Neumar, G. Nichol, D.K. Pandey, N.P. Paynter, M.J. Reeves, P.D. Sorlie, J. Stein, A. Towfighi, T.N. Turan, S.S. Virani, N.D. Wong, D. Woo, M.B. Turner, Heart disease and stroke statistics—2014 update: a report from the American Heart Association, *Circulation* 129 (2014) e28–e292.
- [2] A. Farb, G. Sangiorgi, A.J. Carter, V.M. Walley, W.D. Edwards, R.S. Schwartz, R. Virmani, Pathology of acute and chronic coronary stenting in humans, *Circulation* 99 (1999) 44–52.
- [3] Y.H. Ma, S.Y. Wu, T. Wu, Y.J. Chang, M.Y. Hua, J.P. Chen, Magnetically targeted thrombolysis with recombinant tissue plasminogen activator bound to poly-acrylic acid-coated nanoparticles, *Biomaterials* 30 (19) (2009) 3343–3351.
- [4] S. Lyer, R. Tietze, R. Jurgons, T. Struffert, T. Engelhorn, E. Schreiber, A. Dorfler, C. Alexiou, Visualisation of tumour regression after local chemotherapy with magnetic nanoparticles – a pilot study, *Anticancer Res.* 30 (5) (2010) 1553–1557.
- [5] Y. Zhang, W. Li, L. Ou, W. Wang, E. Delyagina, C. Lux, H. Sorg, K. Riehemann, G. Steinhoff, N. Ma, Targeted delivery of human VEGF gene via complexes of magnetic nanoparticle-adenoviral vectors enhanced cardiac regeneration, *PLoS One* 7 (7) (2012) e39490.
- [6] C. Janko, S. Durr, L.E. Munoz, S. Lyer, R. Chaurio, R. Tietze, S. Lohneisen, C. Schorn, M. Herrmann, C. Alexiou, Magnetic drug targeting reduces the chemotherapeutic burden on circulating leukocytes, *Int. J. Mol. Sci.* 14 (4) (2013) 7341–7355.
- [7] R. Tietze, S. Lyer, S. Durr, T. Struffert, T. Engelhorn, M. Schwarz, E. Eckert, T. Goen, S. Vasylyev, W. Peukert, et al., Efficient drug-delivery using magnetic nanoparticles – biodistribution and therapeutic effects in tumour bearing rabbits, *Nanomedicine* 9 (7) (2013) 961–971.
- [8] I. Cicha, S. Lyer, C. Alexiou, C.D. Garlich, Nanomedicine in diagnostics and therapy of cardiovascular diseases: beyond atherosclerotic plaque imaging, *Nanotechnol. Rev.* 2 (2013) 449–472.
- [9] I. Cicha, C. Garlich, C. Alexiou, Cardiovascular therapy through nanotechnology – how far are we still from bedside? *Eur. J. Nanomed.* 6 (2014) 63–87.
- [10] X. Wu, Y. Tan, H. Mao, M. Zhang, Toxic effects of iron oxide nanoparticles on human umbilical vein endothelial cells, *Int. J. Nanomed.* 5 (2010) 385–399.
- [11] I.M. Kennedy, D. Wilson, A.I. Barakat, Uptake and inflammatory effects of nanoparticles in a human vascular endothelial cell line, *Res. Rep. Health Eff. Inst.* 136 (2009) 3–32.
- [12] I. Cicha, K. Beronov, E. Lopez Ramirez, K. Osterode, M. Goppelt-Struebe, D. Raaz, A. Yilmaz, W.G. Daniel, C.D. Garlich, Shear stress preconditioning modulates endothelial susceptibility to circulating TNF- $\alpha$  and monocytic cell recruitment in a simplified model of arterial bifurcations, *Atherosclerosis* 207 (2009) 93–102.
- [13] S. Dürr, S. Lyer, J. Mann, C. Janko, R. Tietze, E. Schreiber, M. Herrmann, C. Alexiou, Real-time cell analysis of human cancer cell lines after chemotherapy with functionalized magnetic nanoparticles, *Anticancer Res.* 32 (5) (2012) 1983–1989.

- [14] X. Xie, J. Tan, D. Wei, D. Lei, T. Yin, J. Huang, X. Zhang, J. Qiu, C. Tang, G. Wang, *In vitro* and *in vivo* investigations on the effects of low-density lipoprotein concentration polarization and haemodynamics on atherosclerotic localization in rabbit and zebrafish, *J. R. Soc. Interface* 10 (82) (2013) 20121053.
- [15] K. Urschel, C.D. Garlich, W.G. Daniel, I. Cicha, Signalling through vascular endothelial growth factor receptor 2 promotes increased susceptibility to TNF- $\alpha$  in endothelial cells exposed to non-uniform shear stress, *Atherosclerosis* 219 (2011) 499–509.
- [16] K. Urschel, A. Wörner, M. Goppelt-Strube, W.G. Daniel, C.D. Garlich, I. Cicha, Role of shear stress patterns in the TNF- $\alpha$ -induced atherogenic protein expression and monocytic cell adhesion to endothelium, *Clin. Hemorheol. Microcirc.* 46 (2010) 203–210.
- [17] C. Seliger, R. Jurgons, F. Wiekhorst, D. Eberbeck, L. Trahms, H. Iro, C. Alexiou, *In vitro* investigation of the behaviour of magnetic particles by a circulating artery model, *J. Magn. Magn. Mater.* 311 (1) (2007) 358–362.
- [18] R. Tietze, R. Jurgons, S. Lyer, E. Schreiber, F. Wiekhorst, D. Eberbeck, H. Richter, U. Steinhoff, L. Trahms, C. Alexiou, Quantification of drug-loaded magnetic nanoparticles in rabbit liver and tumor after *in vivo* administration, *J. Magn. Magn. Mater.* 321 (10) (2009) 1465–1468.